Evidence for Synergy Between Saccades and Smooth Pursuit During Transient Target Disappearance

Jean-Jacques Orban de Xivry, Simon J. Bennett, Philippe Lefèvre and Graham R. Barnes

JN 95:418-427, 2006. First published Sep 14, 2005; doi:10.1152/jn.00596.2005

J Neurophysiol 95: 418–427, 2006.
First published September 14, 2005; doi:10.1152/jn.00596.2005.

Evidence for Synergy Between Saccades and Smooth Pursuit During Transient Target Disappearance

Jean-Jacques Orban de Xivry,[1,2] Simon J. Bennett,[3] Philippe Lefèvre,[1,2] and Graham R. Barnes[3]
[1]*Center for Systems Engineering and Applied Mechanics, Université catholique de Louvain, Louvain-la-Neuve;* [2]*Laboratory of Neurophysiology, Université catholique de Louvain, Brussels, Belgium; and* [3]*Faculty of Life Sciences, University of Manchester, Manchester, United Kingdom*

Submitted 9 June 2005; accepted in final form 12 September 2005

Orban de Xivry, Jean-Jacques, Simon J. Bennett, Philippe Lefèvre, and Graham R. Barnes. Evidence for synergy between saccades and smooth pursuit during transient target disappearance. *J Neurophysiol* 95: 418–427, 2006. First published September 14, 2005; doi:10.1152/jn.00596.2005. Visual tracking of moving objects requires prediction to compensate for visual delays and minimize mismatches between eye and target position and velocity. In everyday life, objects often disappear behind an occluder, and prediction is required to align eye and target at reappearance. Earlier studies investigating eye motion during target blanking showed that eye velocity first decayed after disappearance but was sustained or often recovered in a predictive way. Furthermore, saccades were directed toward the unseen target trajectory and therefore appeared to correct for position errors resulting from eye velocity decay. To investigate the synergy between smooth and saccadic eye movements, this study used a target blanking paradigm where both position and velocity of the target at reappearance could vary independently but were presented repeatedly to facilitate prediction. We found that eye velocity at target reappearance was only influenced by expected target velocity, whereas saccades responded to the expected change of target position at reappearance. Moreover, subjects exhibited on-line adaptation, on a trial-by-trial basis, between smooth and saccadic components; i.e., saccades compensated for variability of smooth eye displacement during the blanking period such that gaze at target reappearance was independent of the level of smooth eye displacement. We suggest these results indicate that information arising from efference copies of saccadic and smooth pursuit systems are combined with the goal of adjusting eye position at target reappearance. Based on prior experimental evidence, we hypothesize that this spatial remapping is carried out through interactions between a number of identified neurophysiological structures.

INTRODUCTION

Visual tracking of a moving target is a common process in our everyday life. This ability allows us to play sports requiring hitting and catching balls and is also used when navigating within our surrounds (Brouwer et al. 2003; Land and Furneaux 1997; Land and McLeod 2000; Rodrigues et al. 2002; Rushton and Wann 1999). Estimating the final position of moving objects may not always be sufficient to perform these actions because it does not account for unexpected changes in the target motion. Instead, it is typical to continuously predict the target motion to maintain the target image on the fovea. The oculomotor system can achieve this form of prediction using a corollary discharge mechanism (Robinson et al. 1986) that feeds the system with an efference copy of the ongoing eye movement. As well as enabling the oculomotor system to overcome the inherent perceptual-motor delay, prediction is particularly useful when the target moves behind another object. In this case, visual feedback is no longer available to correct for any small mismatch between the eye and object motion, and therefore prediction of occluded target motion is required to minimize position and velocity errors between eye and target at reappearance (Filion et al. 1996).

Visual tracking of a moving target is usually achieved by the collaboration between two oculomotor subsystems: saccades and smooth eye movements (see Krauzlis 2004; Krauzlis and Stone 1999 for reviews). In the event that eye and target position are not perfectly matched, e.g., after an unexpected change in the target path, eye and target have to be realigned. The saccadic system is used to compensate for position mismatch between eye and target by triggering corrective saccades. During visually guided pursuit, the amplitude of catch-up saccades is based on the prediction of the difference between eye and target position at the end of the saccade (de Brouwer et al. 2001, 2002). However, even when the target suddenly disappears, the saccadic system is able to trigger saccades to the expected position of the invisible target (Barborica and Ferrera 2004). Indeed, Filion et al. (1996) showed that primates can approximately predict target position when it has disappeared behind an occluder. The smooth pursuit system is used to compensate for velocity mismatch (i.e., retinal slip) between eye and target and achieves this during visually guided pursuit by increasing gain. However, when the target is occluded and retinal slip is not available, there is an exponential decay of eye velocity (de Brouwer et al. 2001; Pola and Wyatt 1997), which continues to zero if the target is not expected to reappear (Mitrani and Dimitrov 1978). In contrast, when the target is expected to reappear, eye velocity decreases until it reaches a plateau value where it is maintained (Becker and Fuchs 1985; Pola and Wyatt 1997) or recovers in anticipation of target reappearance (Becker and Fuchs 1985; Bennett and Barnes 2003). The eye velocity trajectory during a transient target disappearance can be modeled by a modification of the pursuit gain (Bennett and Barnes 2003, 2004; Churchland et al. 2003; Madelain and Krauzlis 2003) and simulates well the finding that the decrease in eye velocity is dependent on the experience of the subject (Madelain and Krauzlis 2003), and that the scaling of the recovery is modified according to expectation of target velocity at reappearance (Bennett and Barnes (2004).

Address for reprint requests and other correspondence: G. R. Barnes, Moffat Building, PO Box 88, Sackville St., Manchester M60 1QD, UK (E-mail: g.r.barnes@manchester.ac.uk).

The costs of publication of this article were defrayed in part by the payment of page charges. The article must therefore be hereby marked "*advertisement*" in accordance with 18 U.S.C. Section 1734 solely to indicate this fact.

It has also been shown that subjects use a combination of saccades and smooth pursuit to continue eye motion during target blanking. In a recent study, Bennett and Barnes (2005) reported that the saccades were triggered and directed to the expected target position and by generally overshooting they combined with the reduced eye velocity to match the target displacement reasonably well. However, to date, there has been no quantitative analysis of how saccades triggered during target blanking interact with the contribution from the smooth pursuit system. Therefore to examine this issue, we used a target blanking paradigm where both position and velocity of target at reappearance could vary independently. This paradigm allowed us to show that the hypothesized gain increase that elicits the predictive recovery was influenced only by the velocity of the target at reappearance and not by its position. Moreover, we showed that the saccadic system accounted for the target position at reappearance, not velocity, and furthermore that it took into account the variability of the smooth eye displacement. Therefore beside the interaction between saccadic and smooth pursuit systems based on retinal signals, we showed that there is a synergy between both systems when there is no visual input, and hence a combining of information from efference copy of saccadic and smooth eye movements.

METHODS

Experimental set-up

Six healthy human subjects (mean age: 28.7 yr), all of whom had previous experience with ocular pursuit tasks, participated after giving informed consent. All subjects had normal or corrected-to-normal vision, were healthy, and were without any known oculomotor abnormalities. The experiments were carried out according to a protocol approved by the University of Manchester local ethics committee and in accordance with the Declaration of Helsinki.

Subjects sat in a purpose-built dark room, facing a flat white screen (1.5 × 1.5 m) at a viewing distance of 1.7 m. Their head was restrained with head clamps and a chin rest. We projected onto the screen a green fixation target, with a diameter of 0.6° and luminance of 0.5 cd/m^2, and a red pursuit target, consisting of a ring of 12 light-emitting diodes (LEDs) that were optically reduced to form a ring of dots with a diameter of 1.2° and luminance of 0.5 cd/m^2. The green fixation target was illuminated throughout the experimental sessions and remained stationary at a position of –20° to the left of the screen center. The red pursuit target was reflected from a mirror galvanometer, which controlled its horizontal movement across the screen. Visibility of the red pursuit target was controlled by toggling the illumination of the diodes. Eye movements were recorded at 200 Hz using a Chronos eye tracker (Skalar Medical BV), which is based on high-frame rate CMOS sensors (Clarke et al. 2002). The eye tracker has a resolution better than 0.1° in a range of measurement of ±40°. A calibration procedure was performed in which subjects pursued the red target following an ellipsoidal path with horizontal amplitude of 20° and vertical amplitude of 10° at a frequency of 0.195 Hz.

Paradigm

Subjects performed 11 blocks during which they were required to visually track the red pursuit target. Presentations were received in blocks to maximize stimulus predictability and differed according to the visibility of the red pursuit target and its motion characteristics. In the initial part of each presentation, before pursuit target motion onset, subjects were presented with the green fixation target alone at a position located −20° to the left of screen center for 2,000 ms (rest period). An audio cue was given for 80 ms to signal the start of the presentation. The start of the audio cue corresponded to the start of the fixation period, which lasted 400 ms. After this fixation period, the red pursuit target began to move rightward at a velocity of 18°/s.

In the first two blocks, subjects received eight presentations during which the pursuit target was visible for 1,800 ms of constant velocity motion (continuous build-up presentation), followed by eight presentations in which the pursuit target was visible for only 400 ms (interrupted build-up presentation). They received a further nine blocks of 10 presentations, each consisting of 2 continuous build-up presentations, followed by 8 test presentations. In the test presentations, the pursuit target first appeared for a 400-ms ramp but was occluded for a 1,000-ms interstimulus interval (ISI) before reappearing for a further 400-ms ramp motion. All presentations lasted 4,210 ms to give sufficient time for subjects to return their gaze to the green fixation target in preparation for the upcoming presentation.

The target motion characteristics were modified during the ISI such that the target reappeared at one of three possible positions and with one of three possible velocities (Fig. 1). The reappearance positions were computed as if the pursuit target moved from the endpoint of the first 400-ms ramp at a velocity of 12, 18, or 24°/s during the ISI (V_{ISI}). When V_{ISI} was equal to 18°/s, the reappearance position was a simple linear extrapolation from the first ramp and resulted in zero position step. On the other hand, when V_{ISI} was equal to either 12 or 24°/s, the target appeared either closer (negative position step) or further (positive position step) than expected from the extrapolation of the first ramp. By varying V_{ISI}, we effectively created a position step (PS) at the moment of target reappearance of −6, 0, or 6°. A similar procedure was used to generate the velocity step (VS), which thus represented the difference between actual and expected (from the 1st 400 ms, 18°/s) target velocity at reappearance. By modifying target velocity at the moment of reappearance, we created a VS of −6, 0, and 6°/s, which was independent of the reappearance position and hence PS.

To represent all possible combinations of the target motion parameters (3 PSs and 3 VSs), subjects received nine blocks (preceded by 2 blocks of build-up presentations) in a single run of the experiment. A particular combination of these two parameters remained constant within a block, but the order in which they were received was randomized across subjects to minimize sequence effects. The calibration procedure was performed before every four blocks. Three of the subjects performed two runs of the experiment, giving a total of 18 experimental blocks, whereas the other three subjects performed four runs of the experiment giving a total of 36 experimental blocks. Each run of the experiment was performed on a separate day. Subjects were instructed to track the horizontal target as accurately as possible throughout the presentations. They were also told that a block always started with two continuous build-up presentations but they did not know what parameters to expect before the first test presentation of each experimental block.

Data analysis

Eye and target positions were sampled at 200 Hz and stored for off-line analysis with Matlab (Mathworks). Position signals were low-pass filtered using a zero-phase digital filter (autoregressive; forward and backward filter; cut-off frequency, 35 Hz). Eye velocity and acceleration were derived from position signals by means of a central difference algorithm. Saccades were detected using an acceleration threshold of 500°/s^2 and were considered to occur during the ISI if their onset fell 100 ms after the start and before the end of the ISI. Their latency was computed with respect to the start of ISI. Saccades were labeled forward if their velocity peak was in the same direction as the target velocity, otherwise they were labeled as backward. The total contribution of the saccadic system to the displacement during the ISI (SAD) was obtained by summing the signed amplitude of all the saccades. To obtain desaccaded smooth eye

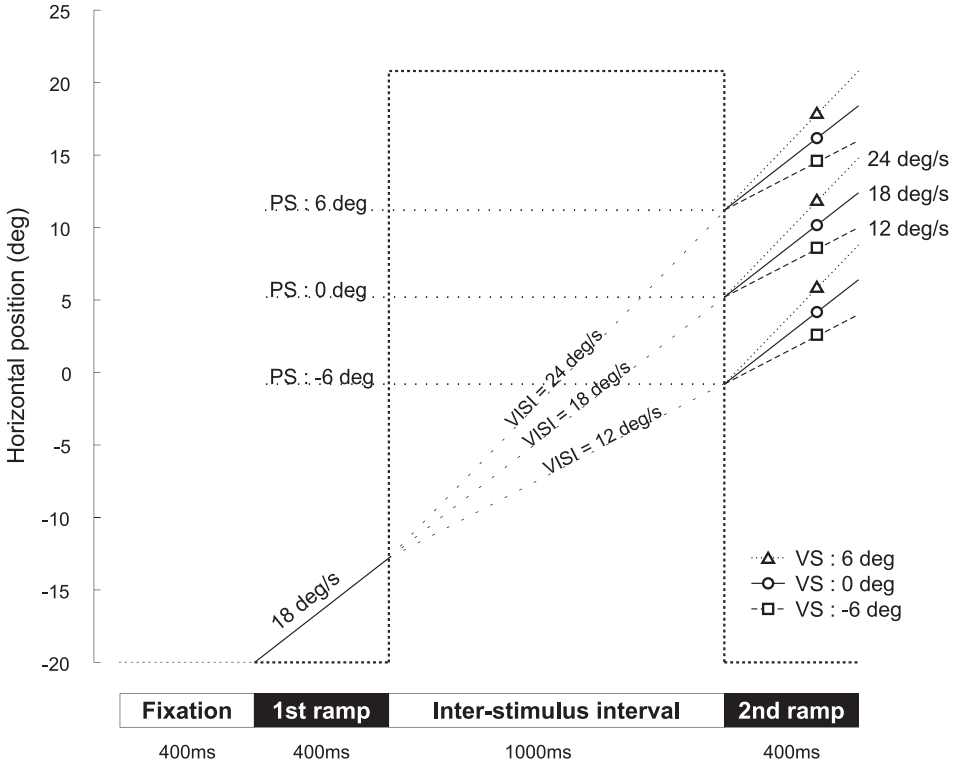

FIG. 1. Representation of pursuit target position vs. time across a presentation. Vertical axis gives horizontal target position (°) and horizontal axis time (ms). When time bar (on the bottom of the graph) is black, red pursuit target was visible. During first ramp interval, target had a constant velocity 18°/s. The interstimulus interval (ISI) is delimited by the light gray dotted line that is low outside ISI and high during ISI. The oblique dashed line represented during ISI gives the 3 possible paths for the virtual target that corresponded to the 3 different position steps (PS). During the 2nd ramp interval, pursuit target path had 9 possible paths, 3 for each possible PS. For 1 given PS, the possible paths were defined by the 3 possible target velocities of the 2nd ramp. Triangle shape superimposed on a dotted line, circle shape superimposed on a continuous line, and square shape superimposed on a dashed line corresponded, respectively, to 2nd ramp velocity of 12, 18, and 24°/s.

velocity, we removed the identified saccades plus an additional five data points (equivalent to 25 ms) at the beginning and end of the identified saccade trajectory from the eye velocity trace. The removed data were replaced by a linear interpolation routine based on the smooth eye velocity before and after the saccade (for more details, see de Brouwer et al. 2002).

To calculate the characteristics of the saccadic movements, we subtracted the contribution of the smooth pursuit system from the saccadic amplitude. The smooth eye displacement during the saccade was obtained by multiplying the estimate of the mean smooth eye velocity during the saccade (obtained by linear interpolation) by its duration. The contribution of the smooth pursuit system to the displacement during the ISI was obtained by integrating the smooth eye velocity during this period.

To compute the magnitude of occurrence of minimum velocity reached during the ISI, we first filtered the desaccaded smooth eye velocity traces at 20 Hz. We then simply searched the eye velocity data during the ISI for the minimum velocity and the corresponding time. The eye velocity data for each presentation were presented on screen and visually inspected, so that when minima were incorrectly identified by the automatic analysis, they could be corrected under interactive control. In some trials, there was no clear minimum velocity during the ISI, and hence no minimum velocity was computed.

We analyzed the steady-state response to the manipulation of target reappearance position and velocity (test presentations 3–8 within each block). To determine if there was an effect of PS and VS on our measures of the smooth and saccadic response, the intrablock mean data for each dependent variable were submitted to separate six subjects by three PS (−6, 0, +6°) by three VS (−6, 0, +6°/s) ANOVA with repeated measures on the last two factors. Where we sought to determine if there was a difference between two separate measures of eye velocity (e.g., eye velocity minimum compared with eye velocity at the moment of target reappearance), these were included as an additional repeated measure in the ANOVA design. Main and interaction effects were further analyzed using Tukey's HSD post hoc procedure (alpha level was $P < 0.05$).

RESULTS

Typical examples

Representative examples of the pursuit response to various test presentations are shown in Fig. 2. As expected given the predictability of the fixation period, subjects exhibited anticipatory eye movements (smooth and saccadic) before the target appeared for the first 400-ms ramp. Eye velocity continued to increase during the first ramp until it matched target velocity. Subjects continued to move their eyes during the ISI, although smooth eye velocity was reduced compared with that in continuous build-up presentations. In general, smooth eye velocity decayed after target offset and recovered to a level that was scaled to target velocity at reappearance (Fig. 2, *A, C*, and *D*). In presentations with a −6°/s VS (Fig. 2*B*), the recovery was represented by a sustained eye velocity at a reduced level. This pattern of decay followed by a scaled recovery during the ISI occurred in 86.4% of all test presentations and confirmed that the response was both anticipatory and predictive of target reappearance. While there was evidence of corrective saccades during the visible portions of the presentations, the reduced smooth eye movements during the ISI were also often combined with one (Fig. 2, *A* and *B*) or several saccades (Fig. 2*D*), despite there being no visual feedback. This was not always the case, and as can be seen for a presentation with a negative position step and positive velocity step (Fig. 2*C*), smooth eye movements alone were sufficient to align gaze to the target position at reappearance. Smooth eye movements alone represented 8% of all the responses ($n = 882$).

Smooth eye velocity

Figure 3 shows a representative example of an individual subject's average eye velocity profiles as a function of the

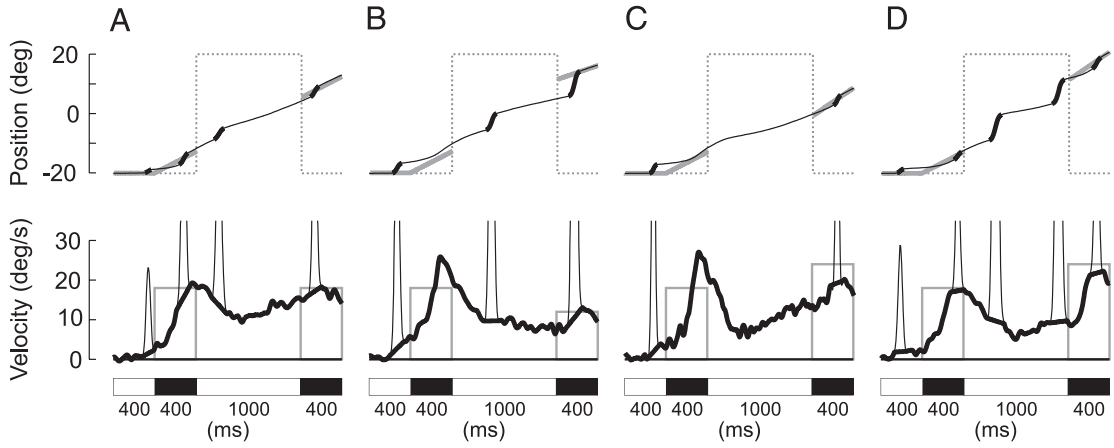

FIG. 2. Representation of eye (black traces) and pursuit target (gray traces) position (°, *top*) and velocity (°/s, *bottom*) vs. time (ms) for 4 typical presentations of a single subject (A, B, C, D) where PS (°) and velocity step (VS; °/s) were equal to (0,0), (6,−6), (−6,6), and (6,6). When time bars (at the base of graphs) are black, pursuit target was visible. On the position panels, thin dotted line is high during ISI and low otherwise; thin eye traces correspond to smooth eye movements; overlaid thick eye traces represent saccades. On the velocity panels, thick eye traces represent desaccaded smooth eye velocity; thin eye traces represent saccades that were removed and replaced by linear interpolation.

different velocity steps for the case where there was no position step; the results were similar for negative and positive position steps. Again, it can be seen that for this subject there was decay in smooth eye velocity during the ISI, which recovered to a level that increased as target velocity at reappearance increased. Note that in the VS = −6° example, eye velocity increased before target onset and decreased toward target velocity. When examined as a group with all individual-subject data pooled together (collapsed across velocity and position steps), the minimum velocity declined to 47% (761 ± 0.01%) of the eye velocity at the beginning of the ISI (17 ± 0.08°/s). In those examples where there was a clear minimum, repeated-measures ANOVA between eye velocity at the start of the ISI and minimum eye velocity indicated that the decay was significant (post hoc Tukey HSD test, $P < 0.05$) for each subject in each condition (except for 1 condition in 1 subject). This decay was neither influenced by PS ($P = 0.27$) nor by VS ($P = 0.47$).

Further ANOVA indicated that there was a significant difference between the eye velocity minimum compared with eye velocity at the moment of target reappearance ($P = 0.0095$). Post hoc analysis (Tukey HSD test) confirmed this effect was evident across each combination of PS and VS in five of the six subjects. It was also confirmed that eye velocity at reappearance was scaled to target velocity [$F(2,878) = 40.92$, $P < 0.0001$], and this effect was present in five of the six subjects (F-test, $P < 0.05$). For a negative VS, eye velocity at target reappearance was approximately equal to target velocity at reappearance (99.7 ± 1.6%), whereas for a zero or positive VS, eye velocity reached 75 ± 1.9% and 66 ± 1.8% of the expected reappearance velocity, respectively (Fig. 4). Therefore, although smooth eye velocity at the moment of target reappearance was scaled to the expected VS, it did not match well the actual target velocity and resulted in considerable retinal slip. As can be seen in Fig. 4, which shows the group mean eye velocity at target reappearance as a function of PS and VS, the scaling of eye velocity at target reappearance was not influenced by PS ($P > 0.12$).

Thus during the ISI, there appeared to be two phases. In the first phase (decay), the smooth eye velocity was neither influenced by PS nor by VS, thus there was no influence of target parameters. In contrast, in the second phase (recovery), which is related to the anticipation of target reappearance, smooth eye velocity at target reappearance was influenced by VS alone. We tested whether the influence of VS on the smooth response occurred at a fixed time during the ISI. To estimate the time when VS begins to influence the smooth response, we performed a Tukey post hoc test on each of the 200 samples along the ISI. For each subject, PS, and sample, we tested whether the mean eye velocities were different between VS = 0 and

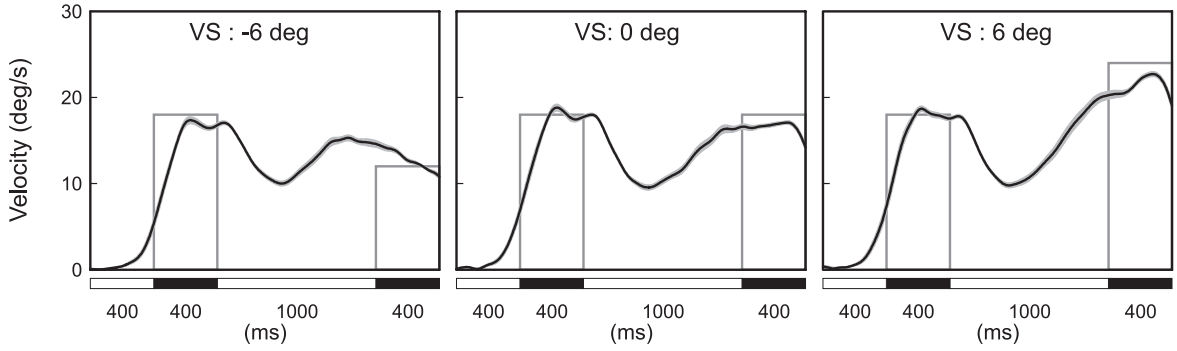

FIG. 3. Representation of the mean eye velocity (°/s) of 1 subject vs. time (ms) for the 3 different VSs when PS was 0 ($V_{ISI} = 18$°/s). Black lines represent mean eye velocity; Dark gray lines represent target velocity; light gray surface around eye velocity traces corresponds to SE. When time bars (*bottom*) are black, pursuit target was visible.

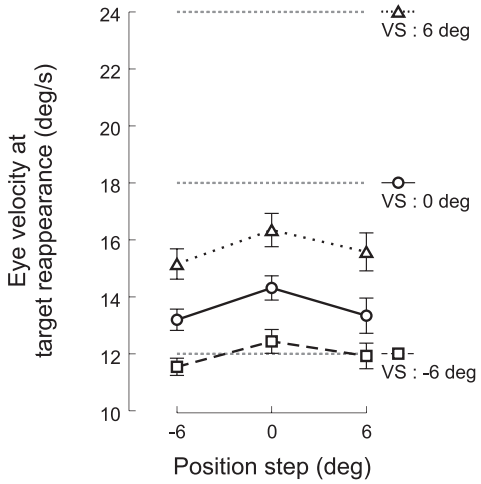

FIG. 4. Eye velocity at target reappearance (°/s) for each combination of PS (horizontal axis) and VS. Triangle shape superimposed on a dotted line, circle shape superimposed on a continuous line, and square shape superimposed on a dashed line correspond, respectively, to 2nd ramp velocity of 12, 18, and 24 °/s. Horizontal gray dotted lines correspond to target velocity at reappearance.

VS = −6, between VS = 0 and VS = 6, and between VS = −6 and VS = 6. We found that the time of divergence varied from 0.2 to 0.9 s from the beginning of the ISI. This shows that there was no clear segregation in the timing of the decay and recovery phases.

Saccades

As previously noted (see Fig. 2, *A, B,* and *D*), saccades also contributed to the eye displacement during the ISI, although observation of the individual-subject data indicated that they appeared less prevalent when there was a negative PS. This could be because fewer saccades were required to match eye displacement to a smaller target displacement during the ISI when PS was negative. To test this hypothesis, we examined the contribution of saccades (i.e., saccadic occurrence, amplitude and endpoint location) to eye displacement during the ISI as a function of PS and VS.

First we found that the number of saccades increased significantly [*F*-test, $F(2,891) = 76.43$, $P < 0.0001$] with PS (on average 1.27, 1.61, and 2.14 saccades per presentation for PS = −6, 0, and 6°), although they were independent of VS. As a consequence, there was an increase in the number of presentations without any saccades as PS decreased. For example, the percentage of presentations in which there was only pure smooth eye movement was 18% when there was a negative PS compared with 5% and 1% when there was a zero or positive PS, respectively. Furthermore, when saccades were separated into two categories (i.e., forward and backward saccades, made in the same or opposite direction to the target), we found that there was a greater percentage of backward saccades (~25% of the total number of saccades) triggered during the ISI when PS was negative. Saccades thus tended to counter the rightward smooth eye displacement to match the expected negative step in target displacement. In contrast, with a positive PS, subjects exhibited more saccades, of which the majority (92%) were forward in the direction of the target. In this case, saccades contributed to the rightward smooth eye displacement as expected target displacement increased.

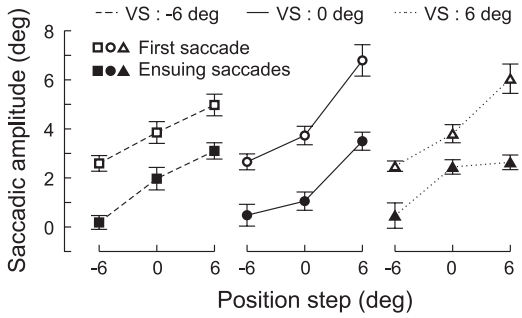

FIG. 5. Average amplitudes (°) of 1st saccades (open symbols) and subsequent saccades (closed symbols) during ISI as a function of PS for each VS. Triangle shape superimposed on a dotted line, circle shape superimposed on a continuous line and square shape, superimposed on a dashed line correspond, respectively, to 2nd ramp velocity of 12, 18, and 24°/s.

Saccadic amplitude (1st and subsequent) was likewise influenced by PS [$F(2,889) = 70.95$, $P < 0.0001$ and $F(2,688) = 66.31$, $P < 0.0001$ for 1st and subsequent saccades, respectively] but was independent of VS [$F(2,889) = 0.4$, $P = 0.67$ and $F(2,688) = 0.47$, $P = 0.62$ for 1st and subsequent saccades, respectively; Fig. 5]. However, the amplitude of the first saccade exhibited during the ISI (Fig. 5, open symbols) was larger than subsequent saccades [closed symbols; *F*-test, $F(1,1581) = 168.05$, $P < 0.0001$]. Forward saccades represented 87, 95, and 98% of the first saccades for negative, zero, and positive PS ($n = 187$, 237, and 237, respectively). Therefore the smaller average amplitudes of subsequent saccades can be explained by the increased proportion of backward saccades as a function of PS [46% (PS = −6, $n = 71$), 22% (PS = 0, $n = 143$), and 14% (PS = 6, $n = 235$), respectively].

The scaling of the saccadic response to PS during the ISI can also be seen in Fig. 6, which shows how the endpoint of saccades fell in the neighborhood of the virtual target path

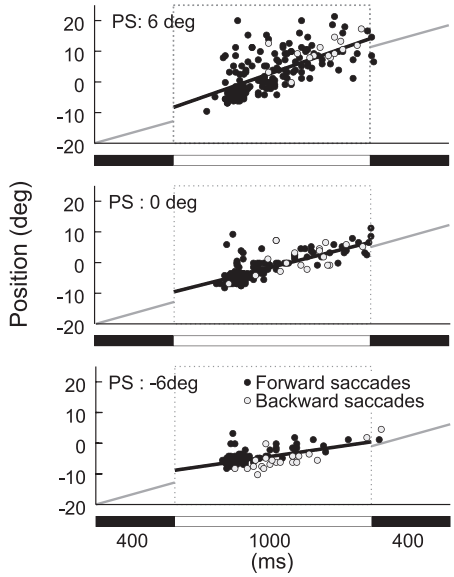

FIG. 6. Offset position (°) from a single subject vs. time (ms) of saccades during ISI for each PS when VS was 0. Closed symbols represent forward saccades and open symbols represent backward saccades. Black oblique lines represent linear best fit. Gray lines correspond to target position before and after ISI. Time bar (*bottom*) is black when pursuit target is present. ISI is delimited by the light gray dotted line that is low outside ISI and high during ISI. Dots beyond the end of the ISI correspond to saccades starting during the ISI.

corresponding to a PS alone (VS of 0°/s). Regression lines appeared to be reasonably parallel to the virtual path that the target would have followed according to the change in V_{ISI} and hence PS, resulting in coefficients for the slope that matched well the unseen target velocity (Table 1). To see if PS or VS and saccadic offset time interact in influencing the saccadic endpoint, we performed a homogeneity-of-slopes test that revealed that the relation between endpoint of saccades and times of saccadic offset was influenced by PS ($P < 0.0001$) but independent of VS ($P = 0.9$). In other words, the slope of the regression lines was dependent on PS and not on VS, as shown in Table 1. To verify that the saccades were directed to the unseen target path and not to a fixed location such as the reappearance target position, we examined the end position of first and ensuing saccades. If these saccades were aimed toward the same fixed location, the end positions should be similar. However, this was not found to be correct; the end position of first and second saccades were significantly different ($P < 0.0001$).

Control of eye displacement

Having shown that the saccadic system adapts to the position step, whereas the smooth pursuit system scales the smooth eye velocity according to the expected target velocity at reappearance (VS), we sought to determine whether the combined response of these two systems led to an eye displacement over the ISI that matched well the target displacement. Figure 7 shows that the total eye displacement (saccades + smooth eye displacement) was, in fact, scaled to the target displacement during ISI. For the three different VSs, there was a very similar pattern of total eye displacement. For a negative PS (black symbols), the position error at the moment of target reappearance was negative, with the eyes ahead of the target by 1.5 ± 0.12° ($n = 290$). When there was no PS (gray symbols), the position error at target reappearance was almost zero (0.15 ± 0.14°; $n = 298$). Finally, for a positive PS (white symbols), the eyes were behind the target, resulting in a position error equal to 1.5 ± 0.23° ($n = 194$). In conclusion, eye displacement during the ISI was influenced by target displacement (ANOVA, $P < 0.0001$) but not by target velocity at reappearance (ANOVA, $P = 0.1$).

TABLE 1. *Parameters related to the regression fit presented in Figure 6*

PS, °	VS, °/s	R	α	β
−6	−6	0.76	−9.8	10.3
−6	0	0.60	−8.8	9.3
−6	6	0.53	−8.3	8.1
0	−6	0.75	−10.2	18.6
0	0	0.76	−9.6	16.3
0	6	0.72	−9.5	16.4
6	−6	0.7	−8.2	20.3
6	0	0.65	−8.3	22.4
6	6	0.78	−9.4	22.7

First and second columns, respectively, represents PS and VS values. Third column shows correlation coefficient. Fourth and fifth columns provide the intercept and slope coefficient of the fit line [$y = \alpha + \beta(t - 0.4)$].

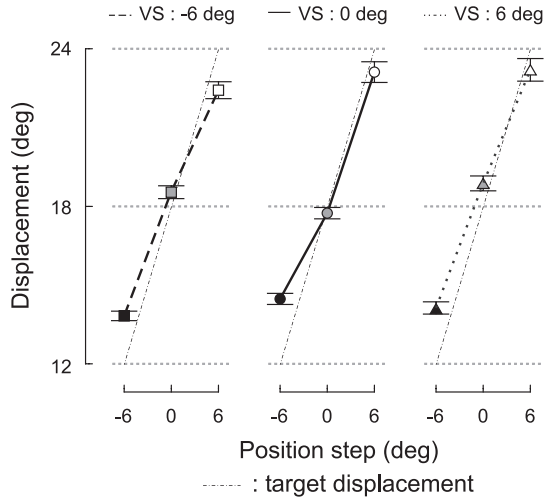

FIG. 7. Eye (dashed, continuous, and dotted lines with symbols) and target (point and bar lines) displacement (°) vs. PS for each VS. Horizontal dotted gray lines correspond to different target displacements. Triangle symbol superimposed on a dotted line, circle symbol superimposed on a continuous line, and square symbol superimposed on a dashed line correspond, respectively, to 2nd ramp velocity of 12, 18, and 24°/s. Black, gray, and white symbols correspond to negative, 0, and positive PSs, respectively.

Interaction between saccadic and pursuit systems

Up to this point we have shown that the contribution from the smooth pursuit and saccadic systems brought gaze to approximately the right position at the right time and with a scaled velocity. However, it remains to be verified if both systems worked in synergy to produce this response. To examine this issue, we performed additional analysis on each individual subject's response to multiple presentations with identical target parameters (e.g., positive PS and VS). Representative data from a single subject are shown in Fig. 8 (I, II, III, and IV; these are selected examples and were not received sequentially). In these examples, the smooth response during the ISI becomes stronger from presentation I to IV, and as a consequence, there are fewer saccades during the ISI in presentation IV than in the other presentations. Additionally, comparison of presentations I–III shows that the saccade amplitudes tend to decrease as smooth response during the ISI increased. Finally, it is noteworthy that in each of these four presentations, there was a relatively small position error at target reappearance. Therefore it would seem that this subject achieved this level of performance using a different combination of smooth eye movements and saccades during the ISI.

To analyze these presentations in more detail, we computed the contribution of both the smooth pursuit [i.e., smooth eye displacement (SED)] and saccadic systems [i.e., saccadic displacement (SAD)] to the eye displacement during the ISI and determined how they covaried. In the examples of Fig. 8, presentations I–IV were ranked in ascending order of SED (9.9, 13.3, 17.8, and 21.1°, respectively). SED was related to the minimum eye velocity reached during the ISI ($r = 0.9$, $P < 0.001$), a smaller minimum occurring with a reduced SED. Conversely, SAD decreased from presentation I to IV (14.6, 9.1, 7.2, and 5.4°, respectively). Therefore the implication is that SED and SAD compensated for each other such that, when there was a smaller (larger) SED, this was matched by a larger (smaller) SAD.

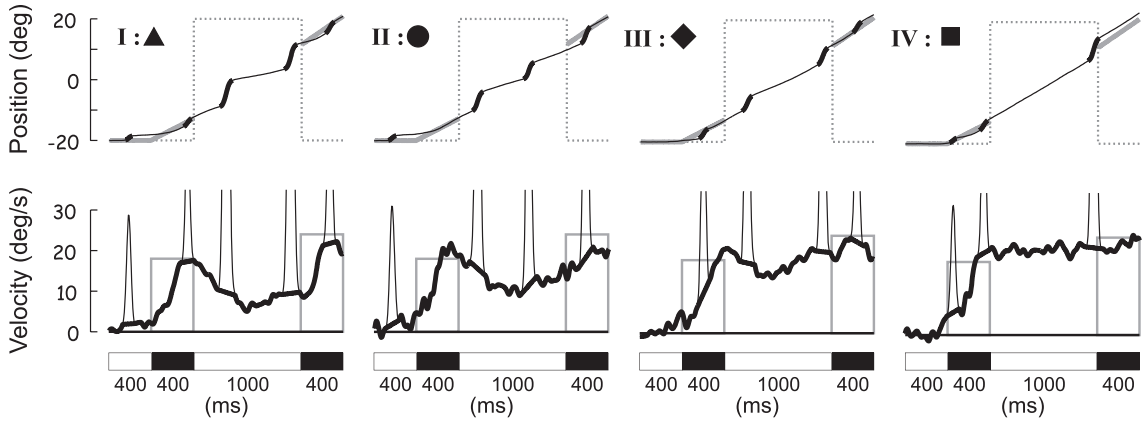

FIG. 8. Representation of eye (black traces) and pursuit target (gray traces), μ position (°, *top*), and velocity (°/s, *bottom*) vs. time (ms) for 4 typical presentations (I, II, III, IV) of the same combination of PS (6°) and VS (6°/s). When time bars (*bottom*) are black, pursuit target was visible. On the position panels, thin dotted line is high during ISI and low outside; thin eye traces correspond to smooth eye movements; and thick eye traces to saccades. On the velocity panels, thick eye traces represent desaccaded smooth eye velocity and thin eye traces represent saccades.

To investigate whether this compensatory role between the smooth and saccadic systems existed across each of the different combinations of PS and VS, we plotted separately for each combination of target parameters the relationship between SED and SAD during the ISI for all subjects' individual presentations (Fig. 9). Focusing on the *top right panel,* which corresponds to a positive PS and VS, and from which examples of Fig. 8 were extracted, regression analysis revealed that the relationship between SED and SAD had a negative trend. The regression equation (for *top right panel*: SAD = 20.3 − 0.65 × SED) gives an idea of the mean compensation between saccadic and smooth pursuit system and shows that, in this case, saccades compensated for 65% of the variation of smooth eye displacement. There was a significant relationship between SAD and SED for all combinations of PS and VS (slope ranging from −0.49 to −0.82; all $P < 0.001$; see Table 2, 1st column), confirming the fact that SED increased as SAD decreased (Table 1). Comparison against the line representing the ideal compensation between SED and SAD (dashed line with a slope of −1) shows that the position error at target reappearance was relatively low.

Although it would appear in Fig. 9 that there is considerable variability in the way participants combine their smooth and saccadic response during the ISI, we found that each subject showed a relationship between these two systems that was reasonably similar to that described in the group data. The correlation and slope coefficients for each subject as a function of PS and VS are given in Table 2. For a zero or positive PS, the relationship between SED and SAD was negative and significant in the majority of the target conditions. However, for a negative PS, the correlation coefficients were rarely significant because the range of the parameters was too small (smaller than for 0 or positive PS, as visible on Fig. 9). Overall, however, these data confirm that each subject exhibited mutual compensation between the smooth pursuit and saccadic system to bring their gaze to the expected position at the expected time of reappearance.

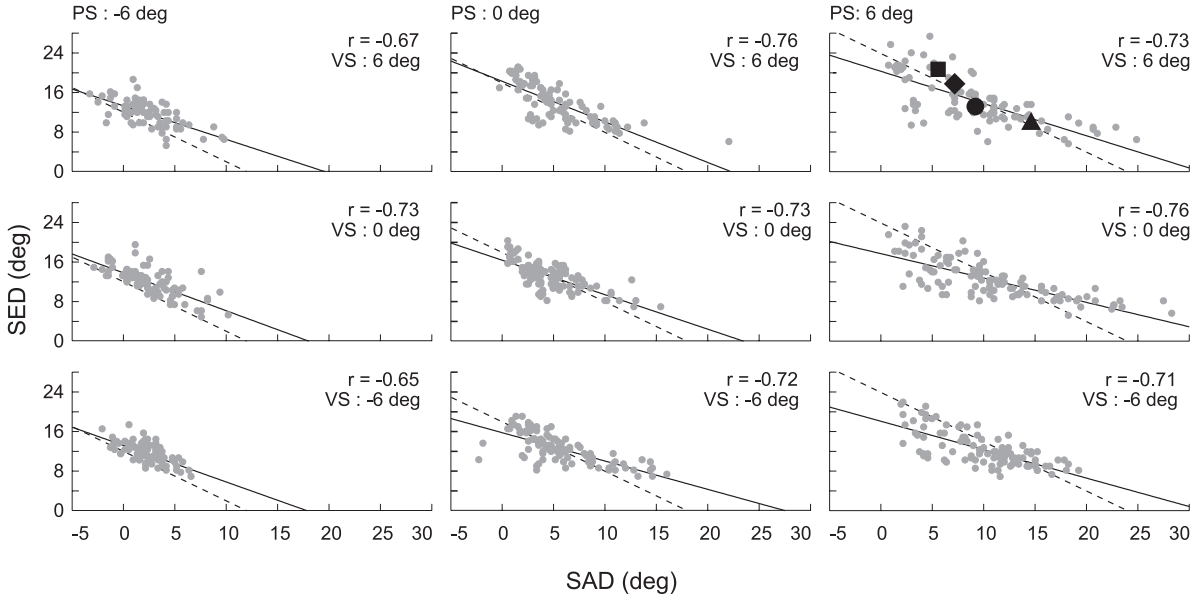

FIG. 9. Scatterplot of smooth eye displacement during ISI (SED, °) vs. sum of saccadic amplitudes (SAD, °) for each combination of PS and VS. Continuous lines represent linear best fit. Dashed lines represent ideal compensation. On the *right top panel*, 4 black symbols correspond to presentations shown in Fig. 8.

TABLE 2. *Correlation (r) and slope (β) coefficients for each target parameter and subject separately*

		Inter subject		S1		S2		S3		S4		S5		S6	
PS	VS	*r*	β	*r*	β	*r*	β	*r*	β	*r*	β	*r*	β	*r*	β
−6	−6	−0.65*	−0.74*	−0.63*	−0.69*	0.07	0.15	0.14	0.3	−0.46	−0.45	−0.4	−0.4	−0.09	−0.07
−6	0	−0.73*	−0.77*	−0.09	−0.1	−0.45	−0.42	0.7*	1.14*	0.17	0.16	−0.67*	−0.84*	0.07	0.04
−6	6	−0.67*	−0.68*	−0.17	−0.29	−0.54*	−0.8*	−0.3	−0.29	−0.6*	−0.42*	−0.64	−0.34	0.84	0.6
0	−6	−0.72*	−0.57*	−0.63*	−0.5*	−0.67*	−0.4*	−0.14	−0.15	−0.71*	−0.26*	−0.15	−0.05	−0.27	−0.13
0	0	−0.73*	−0.7*	−0.49*	−0.38*	−0.56*	−0.4*	−0.41	−0.9	−0.81*	−0.38*	−0.15	0.06	−0.86*	−0.59*
0	6	−0.76*	−0.82*	−0.46*	−0.5*	−0.61*	−0.27*	−0.54*	−0.67*	−0.8*	−0.25*	−0.5	−0.11	−0.93*	−0.68*
6	−6	−0.71*	−0.57*	−0.28	−0.16	−0.64*	−0.21*	−0.8*	−0.59*	−0.4	−0.17	−0.62	−0.2	−0.95*	−0.48*
6	0	−0.76*	−0.49*	−0.82*	−0.46*	−0.62*	−0.16*	−0.49*	−0.39*	−0.73*	−0.28*	−0.51	−0.14	−0.92*	−0.57*
6	6	−0.73*	−0.65*	−0.74*	−0.53*	−0.54*	−0.33*	−0.01	−0.01	−0.78*	−0.34*	0.06	0.03	−0.89*	−0.51*

*Value is significant ($P < 0.05$).

DISCUSSION

In this study, we investigated the ocular pursuit response of human subjects to the transient disappearance of a moving target under conditions where the target reappeared in a predictable way at a different velocity and/or different position to that expected from the first part of the motion. This enabled us to examine independently the response of the smooth and saccadic systems to different but predictable combinations of target position and velocity steps. In line with previous studies (Bennett and Barnes 2005), we observed that a combination of smooth pursuit eye movements and saccades was made in response to the disappearance of a moving target. The smooth pursuit component of this response, which has been studied in cats (de Brouwer et al. 2001), monkeys (Churchland et al. 2003; Kawano et al. 1994), and humans (Becker and Fuchs 1985; Bennett and Barnes 2003; Madelain and Krauzlis 2003), decayed after target disappearance and recovered to a level that was scaled to the expected target velocity (Bennett and Barnes 2004). However, there was no effect of a predictable velocity step on the discrete measures of the saccadic response. In addition, we found that the discrete measures of the smooth pursuit response during the transient (e.g., eye velocity minimum) were not influenced by the predictable position step, and hence, change in target reappearance position. Rather, subjects modified their saccadic response to deal with the predictable position step and hence the change in eye displacement required to align gaze at the moment of target reappearance. For example, when the target reappeared with a −6° position step, more saccades were made in the direction opposite to the smooth eye movement (backward saccades). In contrast, when the target appeared with a 6° position step, saccadic amplitudes were larger and mainly forward in the direction of the smooth eye movement.

Initially, it appeared that given predictable changes in target parameters during the transient, the resulting smooth eye velocity was dependent on target velocity and independent of target position, whereas the saccadic response was dependent on target position and independent of target velocity. Our data thus shed light on an important issue related to the influence of position and velocity steps on smooth pursuit during transient target disappearance. Contemporary models of pursuit assume that target disappearance causes a modification of the gain of the internal efference copy feedback loop, which is responsible for the decay and subsequent recovery of smooth eye velocity (Bennett and Barnes 2003, 2004; Churchland et al. 2003; Madelain and Krauzlis 2003). The decrease in gain to a nonzero value enables smooth eye velocity to be maintained at a reduced level, as observed experimentally (Becker and Fuchs 1985). To obtain a predictive reacceleration, it is necessary to assume that this gain is then predictively increased before target reappearance. The fact that eye velocity at reappearance is independent of the position step implies that the gain increase is dependent on expected target velocity at reappearance and not on expected target position.

The foregoing evidence gives the impression that the saccadic and smooth pursuit systems appear to be independent and aim to achieve different goals. However, in other contexts, both systems have been shown to collaborate in achieving a common goal. Indeed, retinal slip (velocity error) is used by the saccadic system to compute saccadic amplitude by taking eye and target velocity into account (de Brouwer et al. 2001, 2002). In this study, we also showed that eye displacement matched target displacement in an efficient way, indicating that the addition of the responses of both systems yields an appropriate result. This occurs despite the large variability of the smooth response across trials for the same target parameters. Thus we further investigated this interaction to determine whether there was compensation between the smooth and saccadic systems across individual trials. This revealed that the saccadic and smooth pursuit systems worked in synergy during target blanking. Indeed, although there was a tendency to maintain the smooth eye velocity during the occlusion interval, there was considerable variability in the smooth response from one presentation to another. In response to this variability, we found that the saccadic system modified its contribution to the total eye displacement to compensate for changes in the smooth eye displacement (see Fig. 9). Whatever the magnitude of the smooth eye movement, corrective saccades tended to allow the overall eye displacement to closely match target displacement. Thus when smooth pursuit eye movements contributed less to the eye displacement during the ISI (quantified by the smooth eye displacement), the saccadic system increased its contribution. On average 65% of smooth eye displacement variability was taken into account by the saccadic system. This compensation for the variability of the smooth response occurred without any visual feedback, which suggests that extraretinal signals derived from efference copy of smooth eye velocity are available to the saccadic system. This hypothesis is supported by Blohm et al. (2005), who suggested that an efference copy of the smooth eye displacement is available to the saccadic system during a target localization task. These authors showed that, when a target is flashed during smooth pursuit, the

saccadic system can compensate for the smooth eye displacement that takes place after the moving target disappears and maintain space constancy. Interestingly, Blohm et al. (2005) reported that, on average, a similar proportion of smooth eye displacement (55%) was taken into account.

In the experiment of Blohm et al., the eye was directed toward a single point in space, whereas in this experiment, the eye appeared to be directed toward the continuing trajectory of the target, even though that target could not be seen. This implies that the subjects have access to an internal representation of the expected target trajectory and that they are able to compare this with an internal representation of eye position so as to make corrective saccades that will minimize the difference between them. An alternative and simpler hypothesis might be that subjects learned the timing and position of target reappearance in allocentric coordinates and that they used this to compensate for any variability in their smooth eye movements. However, in this case, it might be expected that the oculomotor system would release one corrective saccade toward the end of the ISI rather than multiple saccades (both forward and backward) throughout the ISI. The finding that saccades occurred throughout the ISI and that the endpoints of first and subsequent saccades were significantly different argues against this conclusion. Moreover, even if the subject did operate on the basis of directing gaze toward the target reappearance position during target blanking, the saccadic system would still need an internal representation of concurrent eye position to trigger well-fitted saccades.

Neurophysiological substrate

The smooth pursuit system of nonhuman primates is known to depend on several cortical areas, of which the most studied are the middle temporal (MT) and medial superior temporal (MST) areas (for review, see Krauzlis 2004). MT and MST receive retinal velocity error signals from the primary visual cortex (V1), but MST also receives extraretinal inputs that are necessary to maintain smooth pursuit eye movement during transient disappearance of the target (Ilg and Thier 2003; Kawano et al. 1994; Newsome et al. 1988). Extraretinal signals were also found in the ventral intraparietal area (VIP), which is highly connected with MST (Schlack et al. 2003) and in the frontal eye field (FEF) (Barborica and Ferrera 2003; Fukushima et al. 2002), which also communicates with MST. Apart from the role of FEF in the saccadic system, an adjacent region of FEF is also involved in smooth pursuit (Tanaka and Fukushima 1998; Tanaka and Lisberger 2002a,b) and has been associated with the regulation of pursuit gain (Lekwuwa and Barnes 1996a,b; Tanaka and Lisberger 2001). Activation of this cortical network during pursuit eye movements has been described in several functional MRI studies in humans (Lencer et al. 2004; O'Driscoll et al. 2000; Petit and Haxby 1999; Schmid et al. 2001).

In one such study, Lencer et al. (2004) reported that among other areas, FEF and LIP remained activated in humans during target blanking. This is consistent with findings in monkeys by Barborica and Ferrera (2004), who showed that activity in FEF is related to target velocity during fixation and, moreover, is maintained during target blanking. In addition, these authors showed that the monkeys were able to make a corrective saccade to the predicted position of the target at reappearance; this was taken to indicate that the activity in FEF might be integrated to obtain a representation of the unseen target trajectory. Extending on this, Bennett and Barnes (2005) proposed that, even when the eye is in motion and there is no visual feedback, the target velocity-related activity in FEF could be derived from extraretinal input. Integration of this signal would provide a continuous internal representation of expected target trajectory, as described earlier. This could be compared with an internal representation of eye position and used by the saccadic system to trigger saccades directed toward the unseen target trajectory. It is noteworthy, however, that this representation of eye position should ideally take account of the combination of prior smooth and saccadic eye movements.

At present, the form of this internal representation is unknown. It could be a single position-coded signal derived from the brain stem or alternatively it might be derived from the combination of separate representations of smooth and saccadic components further upstream. The likely recipient of this position-coded signal (Bremmer et al. 1997) is area LIP, which has an established role in remapping the visual scene when keeping track of saccades (Duhamel et al. 1992; Heide et al. 2001; Medendorp et al. 2003) and of smooth pursuit eye movements or the vestibulo-ocular reflex (Powell and Goldberg 1997; Snyder 2000; Snyder and Harper 1999), and could thus keep track of self-motion as proposed by Blohm et al. (2005). We suggest that LIP is thus the most likely area where internal signals representing the continuing target trajectory and current position are compared during target blanking for the purpose of deriving corrective saccades.

GRANTS

This work was supported by the Leverhulme Trust (UK); the Medical Research Council (UK); the Fonds National de la Recherche Scientifique; the Fondation pour la Recherche Scientifique Médicale; the Belgian Program on Interuniversity Attraction Poles initiated by the Belgian Federal Science Policy Office; internal research grant (Fonds Spéciaux de Recherche) of the Université Catholique de Louvain; and the European Space Agency (ESA) of the European Union. The scientific responsibility rests with its authors.

REFERENCES

Barborica A and Ferrera VP. Estimating invisible target speed from neuronal activity in monkey frontal eye field. *Nat Neurosci* 6: 66–74, 2003.

Barborica A and Ferrera VP. Modification of saccades evoked by stimulation of frontal eye field during invisible target tracking. *J Neurosci* 24: 3260–3267, 2004.

Becker W and Fuchs AF. Prediction in the oculomotor system: smooth pursuit during transient disappearance of a visual target. *Exp Brain Res* 57: 562–575, 1985.

Bennett SJ and Barnes GR. Human ocular pursuit during the transient disappearance of a visual target. *J Neurophysiol* 90: 2504–2520, 2003.

Bennett SJ and Barnes GR. Predictive smooth ocular pursuit during the transient disappearance of a visual target. *J Neurophysiol* 92: 578–590, 2004.

Bennett SJ and Barnes GR. Combined smooth and saccadic ocular pursuit during the transient occlusion of a moving visual object. *Exp Brain Res* In press.

Blohm G, Missal M, and Lefevre P. Processing of retinal and extraretinal signals for memory-guided saccades during smooth pursuit. *J Neurophysiol* 93: 1510–1522, 2005.

Bremmer F, Distler C, and Hoffmann K-P. Eye position effects in monkey cortex. II. Pursuit- and fixation-related activity in posterior parietal areas LIP and 7A. *J Neurophysiol* 77: 962–977, 1997.

Brouwer AM, Middelburg T, Smeets JB, and Brenner E. Hitting moving targets: a dissociation between the use of the target's speed and direction of motion. *Exp Brain Res* 152: 368–375, 2003.

Churchland MM, Chou IH, and Lisberger SG. Evidence for object permanence in the smooth-pursuit eye movements of monkeys. *J Neurophysiol* 90: 2205–2218, 2003.

Clarke AH, Ditterich J, Druen K, Schonfeld U, and Steineke C. Using high frame rate CMOS sensors for three-dimensional eye tracking. *Behav Res Methods Instrum Comput* 34: 549–560, 2002.

de Brouwer S, Missal M, Barnes G, and Lefevre P. Quantitative analysis of catch-up saccades during sustained pursuit. *J Neurophysiol* 87: 1772–1780, 2002.

de Brouwer S, Missal M, and Lefèvre P. Role of retinal slip in the prediction of target motion during smooth and saccadic pursuit. *J Neurophysiol* 86: 550–558, 2001.

Duhamel JR, Colby CL, and Goldberg ME. The updating of the representation of visual space in parietal cortex by intended eye movements. *Science* 255: 90–92, 1992.

Filion CM, Washburn DA, and Gulledge JP. Can monkeys (Macaca mulatta) represent invisible displacement? *J Comp Psychol* 110: 386–395, 1996.

Fukushima K, Yamanobe T, Shinmei Y, and Fukushima J. Predictive responses of periarcuate pursuit neurons to visual target motion. *Exp Brain Res* 145: 104–120, 2002.

Heide W, Binkofski F, Seitz RJ, Posse S, Nitschke MF, Freund HJ, and Kompf D. Activation of frontoparietal cortices during memorized triple-step sequences of saccadic eye movements: an fMRI study. *Eur J Neurosci* 13: 1177–1189, 2001.

Ilg UJ and Thier P. Visual tracking neurons in primate area MST are activated by smooth-pursuit eye movements of an "imaginary" target. *J Neurophysiol* 90: 1489–1502, 2003.

Kawano K, Shidara M, Watanabe Y, and Yamane S. Neural activity in cortical area MST of alert monkey during ocular following responses. *J Neurophysiol* 71: 2305–2324, 1994.

Krauzlis RJ. Recasting the smooth pursuit eye movement system. *J Neurophysiol* 91: 591–603, 2004.

Krauzlis RJ and Stone LS. Tracking with the mind's eye. *Trends Neurosci* 22: 544–550, 1999.

Land MF and Furneaux S. The knowledge base of the oculomotor system. *Philos Trans R Soc Lond B Biol Sci* 352: 1231–1239, 1997.

Land MF and McLeod P. From eye movements to actions: how batsmen hit the ball. *Nat Neurosci* 3: 1340–1345, 2000.

Lekwuwa GU and Barnes GR. Cerebral control of eye movements. I. The relationship between cerebral lesion sites and smooth pursuit deficits. *Brain* 119: 473–490, 1996a.

Lekwuwa GU and Barnes GR. Cerebral control of eye movements. II. Timing of anticipatory eye movements, predictive pursuit and phase errors in focal cerebral lesions. *Brain* 119: 491–505, 1996b.

Lencer R, Nagel M, Sprenger A, Zapf S, Erdmann C, Heide W, and Binkofski F. Cortical mechanisms of smooth pursuit eye movements with target blanking. An fMRI study. *Eur J Neurosci* 19: 1430–1436, 2004.

Madelain L and Krauzlis RJ. Effects of learning on smooth pursuit during transient disappearance of a visual target. *J Neurophysiol* 90: 972–982, 2003.

Medendorp WP, Goltz HC, Vilis T, and Crawford JD. Gaze-centered updating of visual space in human parietal cortex. *J Neurosci* 23: 6209–6214, 2003.

Mitrani L and Dimitrov G. Pursuit eye movements of a disappearing moving target. *Vision Res* 18: 537–539, 1978.

Newsome WT, Wurtz RH, and Komatsu H. Relation of cortical areas MT and MST to pursuit eye movements. II. Differentiation of retinal from extraretinal inputs. *J Neurophysiol* 60: 604–620, 1988.

O'Driscoll GA, Wolff AL, Benkelfat C, Florencio PS, Lal S, and Evans AC. Functional neuroanatomy of smooth pursuit and predictive saccades. *Neuroreport* 11: 1335–1340, 2000.

Petit L and Haxby JV. Functional anatomy of pursuit eye movements in humans as revealed by fMRI. *J Neurophysiol* 82: 463–471, 1999.

Pola J and Wyatt HJ. Offset dynamics of human smooth pursuit eye movements: effects of target presence and subject attention. *Vision Res* 37: 2579–2595, 1997.

Powell K and Goldberg ME. Remapping of visual responses in primate parietal cortex during smooth changes in gaze. *Soc Neurosci Abstr* 23: 17, 1997.

Robinson DA, Gordon JL, and Gordon SE. A model of the smooth pursuit eye movement system. *Biol Cybern* 55: 43–57, 1986.

Rodrigues ST, Vickers JN, and Williams AM. Head, eye and arm coordination in table tennis. *J Sports Sci* 20: 187–200, 2002.

Rushton SK and Wann JP. Weighted combination of size and disparity: a computational model for timing a ball catch. *Nat Neurosci* 2: 186–190, 1999.

Schlack A, Hoffmann KP, and Bremmer F. Selectivity of macaque ventral intraparietal area (area VIP) for smooth pursuit eye movements. *J Physiol* 551: 551–561, 2003.

Schmid A, Rees G, Frith C, and Barnes G. An fMRI study of anticipation and learning of smooth pursuit eye movements in humans. *Neuroreport* 12: 1409–1414, 2001.

Snyder L and Harper T. The representation of spatial information in monkey lateral intraparietal area (LIP) depends on the task being performed. *Soc Neurosci Abstr* 25: 1547, 1999.

Snyder LH. Coordinate transformations for eye and arm movements in the brain. *Curr Opin Neurobiol* 10: 747–754, 2000.

Tanaka M and Fukushima K. Neuronal responses related to smooth pursuit eye movements in the periarcuate cortical area of monkeys. *J Neurophysiol* 80: 28–47, 1998.

Tanaka M and Lisberger SG. Regulation of the gain of visually guided smooth-pursuit eye movements by frontal cortex. *Nature* 409: 191–194, 2001.

Tanaka M and Lisberger SG. Role of arcuate frontal cortex of monkeys in smooth pursuit eye movements. I. Basic response properties to retinal image motion and position. *J Neurophysiol* 87: 2684–2699, 2002a.

Tanaka M and Lisberger SG. Role of arcuate frontal cortex of monkeys in smooth pursuit eye movements. II. Relation to vector averaging pursuit. *J Neurophysiol* 87: 2700–2714, 2002b.